

PAPER

Design and evaluation of a high sensitivity spiral TDR scour sensor

To cite this article: Quan Gao and Xiong (Bill) Yu 2015 *Smart Mater. Struct.* **24** 085005

Manuscript version: Accepted Manuscript

Accepted Manuscript is “the version of the article accepted for publication including all changes made as a result of the peer review process, and which may also include the addition to the article by IOP Publishing of a header, an article ID, a cover sheet and/or an ‘Accepted Manuscript’ watermark, but excluding any other editing, typesetting or other changes made by IOP Publishing and/or its licensors”

This Accepted Manuscript is© .

During the embargo period (the 12 month period from the publication of the Version of Record of this article), the Accepted Manuscript is fully protected by copyright and cannot be reused or reposted elsewhere.

As the Version of Record of this article is going to be / has been published on a subscription basis, this Accepted Manuscript will be available for reuse under a CC BY-NC-ND 3.0 licence after the 12 month embargo period.

After the embargo period, everyone is permitted to use copy and redistribute this article for non-commercial purposes only, provided that they adhere to all the terms of the licence <https://creativecommons.org/licenses/by-nc-nd/3.0>

Although reasonable endeavours have been taken to obtain all necessary permissions from third parties to include their copyrighted content within this article, their full citation and copyright line may not be present in this Accepted Manuscript version. Before using any content from this article, please refer to the Version of Record on IOPscience once published for full citation and copyright details, as permissions may be required. All third party content is fully copyright protected, unless specifically stated otherwise in the figure caption in the Version of Record.

View the [article online](#) for updates and enhancements.

Manuscript version: Accepted Manuscript

The “**Accepted Manuscript**” is the author’s original version of an article including any changes made following the peer review process but excluding any editing, typesetting or other changes made by IOP Publishing and/or its licensors.

During the embargo period (the 12 month period from publication of the Version of Record of this article), the Accepted Manuscript:

- is fully protected by copyright and can only be accessed by subscribers to the journal;
- cannot be reused or reposted elsewhere by anyone unless an exception to this policy has been agreed in writing with IOP Publishing



As the Version of Record of this article is going to be/has been published on a subscription basis, this Accepted Manuscript will be available for reuse under a [CC BY-NC-ND 3.0](#) licence after a 12 month embargo period.

After the embargo period, everyone is permitted to copy and redistribute this article for Non-Commercial purposes only, provided they*:

- give appropriate credit and provide the appropriate copyright notice;
- show that this article is published under a CC BY-NC-ND 3.0 licence;
- provide a link to the CC BY-NC-ND 3.0 licence;
- provide a link to the Version of Record;
- do not use this article for commercial advantage or monetary compensation; and
- only use this article in its entirety and do not make derivatives from it.

*Please see CC BY-NC-ND 3.0 licence for full terms.

View the Version of Record for this article online at iopscience.org

Design and Evaluation of A High Sensitivity Spiral TDR Scour Sensor

Quan Gao¹ Xiong (Bill) Yu^{2*}

¹ Ph.D. candidate, Department of Civil Engineering, Case Western Reserve University, 2104 Adelbert Road, Bingham 211A, Cleveland, OH 44106-7201, qxg29@case.edu.

^{2*} Associate Professor, Department of Civil Engineering, Case Western Reserve University, 2104 Adelbert Road, Bingham 206, Cleveland, OH 44106-7201, xyy21@case.edu, Corresponding Author.

ABSTRACT

Bridge scour accounts for more than half of the reported bridge failures in U.S.. Scour monitoring technology based on time domain reflectometry (TDR) feature the advantages of being automatic and inexpensive. The senior author’s team has developed a few generations of TDR bridge scour monitoring system, which have succeeded in both laboratory and field evaluations. In this study, an innovative spiral TDR sensor is proposed to further improve the sensitivity of TDR sensor in scour detection. The spiral TDR sensor is made of parallel copper wire waveguide wrapped around a mounting rod. By using a spiral path for the waveguide, the TDR sensor achieves higher sensitivity than the traditional straight TDR probes due to longer travel distance of the electromagnetic (EM) wave per unit length in the spiral probe versus traditional probe. The performance of the new TDR spiral scour sensor is validated by calibration with liquids with known dielectric constant and wet soils. Laboratory simulated scour/refilling experiments are performed to evaluate the performance of the new spiral probe in detecting the sediment/water interface and therefore the scour/refill process. The tests results indicate that scour depth variation of less than 2 cm can be easily detected by this new spiral sensor. A theory is developed based on the dielectric mixing model to simplify the TDR signal analyses for scour depth detection. The sediment layer thickness (directly related to scour depth) varies linearly with the square root of bulk dielectric constant of water-sediment mixture measured by the spiral TDR probe, which matches the results of theoretical prediction. The estimated sediment layer thickness and therefore scour depth from the spiral TDR sensor agrees very well with that by direct physical measurement. The spiral TDR sensor is 4 times more sensitive than a traditional straight TDR probe.

KEYWORDS: Time Domain Reflectometry; bridge scour; sensor; TDR probe; spiral TDR probe; Sensitivity.

INTRODUCTION

Bridge scour has been found to cause majority of bridge failures in the United States over the past 40 years (Briaud et al. 2011; Briaud et al. 2005; Briaud et al. 2001; Prendergast and Gavin 2014). The scour around bridge foundation compromise its capability to support the superstructures and lead to bridge collapse in the extreme cases (e.g., flood). Based on the National Cooperative Highway Research Program (NCHRP) report, almost 60% of the reported bridge failures were caused by bridge scour during 1966-2005 (Hunt 2009; Yu and Zabilansky 2006).

The bridge failures induce millions of economic loss in United States every year due to direct cost of restoring and repairing these bridges as well as indirect cost associated with transportation system disruption (Yu et al. 2013). Around 26,000 bridges in the United States are categorized as “scour critical” (Briaud et al. 2011). Therefore, deploying scour countermeasures including monitoring scour is imperative to prevent the catastrophic consequences due to scour induced bridge failures.

Three options are generally applied to mitigate the bridge scour and associated economic losses and casualties, i.e., structural, hydraulic, and monitoring countermeasures (Briaud et al. 2011; Hunt 2009). Monitoring or surveillance using sensing instruments, is considered to be the most effective and efficient method to mitigate the risk of bridge failure or reduce the cost for bridge maintenance, especially for the existing bridges (Prendergast and Gavin 2014).

Existing methods for monitoring bridge scour include the use of conventional techniques, such as “floated out” devices and tethered buried switches (Briaud et al. 2011; Hunt 2009), fiber-Bragg grating sensors (Lin et al. 2005; Lin et al. 2004; Sohn et al. 2004; Xiong et al. 2012), ground penetrating radar (GPR) (Anderson et al. 2007; Forde et al. 1999), sonar (De Falco and Mele 2002; Hayes and Drummond 1995; Mason and Sheppard 1994), sliding collar (Yankielun and Zabilansky 1999) and dropping weights (Lefter 1993), etc. Other methods evaluated in the field include those based on wireless monitoring system, neutral buoyancy “fish” and “smart rocks” as described by Zabilansky (1996) and Radchenko et al. (2013). These technologies have inherent advantages and limitations in certain aspects. For example, GPR requires manual operation and is difficult to use during heavy-flood events when scouring is often at its highest risk of occurrence (Prendergast and Gavin 2014). Sonar is relatively easy to install, but the measuring signals are complex to analyze and interpret and the measurement is highly influenced by the turbidity of stream (Lin et al. 2005; Lin et al. 2004; Xiong et al. 2012; Yu et al. 2013). While progresses are being made over the years, the size, cost, sacrificial nature, and power supply demand remains a challenge for “fish” and “smart rocks” technologies.

Time Domain Reflectometry (TDR) features the advantages of being automatic, real time and inexpensive for the surveillance of bridge scour (Yankielun and Zabilansky 1999; Yu 2009). Yu (2009) studied the feasibility of using traditional 3-rod stainless steel TDR probe for scouring measurement and develop an algorithm for signal analyses. The subsequent study by Bin et al. (2010) developed a flat TDR strip to

facilitate field installation. These previous studies proved the capability of TDR to reliably monitor the scour development. To further improve the accuracy and sensitivity of TDR scour measurement, this paper proposed a new spiral TDR probe made of parallel copper wires waveguide wrapped around a supporting rod. The spiral TDR probe is firstly calibrated using liquid with known dielectric constant and soils with different moisture contents. Its performance was then evaluated using simulated scour experiments. The results show that the spiral TDR probe achieved a much higher resolution in scour depth detection than conventional straight TDR probe.

THEORY OF TIME DOMAIN REFLECTOMETRY (TDR)

Fig. 1(a) shows the schematic of a TDR system, which typically consists of a pulse generator, coaxial cable, a sensing probe and control station such as by PDA, laptop or datalogger. The pulse generator produces a fast rising TDR pulse (with rise time of hundred picoseconds to allow for high resolution in interface detection). Electromagnetic (EM) wave will be reflected back at the air-soil interface and probe end when it is propagated from the generator to the TDR probe (Ledieu et al. 1986; Yu and Drnevich 2004). These reflections are illustrated in Fig. 1 (b).

The EM wave propagation velocity, v , in the media surrounding TDR probe can be determined by equation (1):

$$v = \frac{c}{\sqrt{K_a}} \quad (1)$$

where c is the velocity of an electromagnetic wave in free space ($2.998 \times 10^8 m/s$); K_a is the dielectric constant of material. The dielectric constant of water is around 81 at 20°C. The electric constant of soil solids are around 3-5 and that of the air is around 1.

The time for the signal to round trip in the TDR probe is given by equation (2), provided that the length of probe in the soil is assumed to be L_p .

$$t = \frac{2L_p}{v} \quad (2)$$

Submitting equation (1) into (2) and defining apparent length, $L_a = ct/2$, equation (2) yields

$$K_a = \left(\frac{L_a}{L_p} \right)^2 \quad (3)$$

From this, the dielectric properties of material can be determined from TDR signal.

MIXING FORMULA FOR THE DIELECTRIC CONSTANT

Birchak et al. (1974) proposed a semi-empirical volumetric mixing model to correlate the bulk dielectric constant of a mixture to its components (i.e., equation (4)).

$$(K_m)^\alpha = \sum_{i=1}^n v_i (K_i)^\alpha \quad (4)$$

where v_i and K_i are the volumetric fraction and dielectric permittivity of each component. Since soil is typically considered as a three-phase system, i.e., solid particles as skeleton, air and water in the porous space, the dielectric property of the

soil consists of three components. Birchak et al. (1974) and Ledieu et al. (1986) suggested that the exponent α can be empirically chosen as $\alpha = 0.5$ for geotechnical applications.

For the special case of binary co-solvent (i.e., mixture of two different liquids which was used in the calibration of the TDR probe in this study), the volume of the phases is described by the relationship: $v_2 = 1 - v_1$. The dielectric property for binary co-solvent is very complicated due to intermolecular interactions between each component. Numerous models have been proposed to determine the dielectric constant of solvent mixtures (Amirjahed and Blake 1974; Chien 1984; Dumanovic et al. 1992; Joshi et al. 2011; Jouyban et al. 2004; King and Queen 1979; Prakongpan and Nagai 1984). In this study, dielectric relaxation effect is neglected (Joshi et al. 2011). Equation (4) is used to describe the dielectric constant of ethanol-deionized water mixture, but the value of α is assumed to be 1.0 based on previous studies (Chien 1984; Dumanovic et al. 1992; Jouyban et al. 2004; Prakongpan and Nagai 1984).

PRINCIPLE OF BRIDGE SCOUR DEPTH ESTIMATION

Fig. 2 shows schematic diagram of estimating bridge scour using TDR technology. Water and saturated soil are prepared in a tank with increasing/decreasing thickness of soil layer to simulate the sediment/scour process. TDR signals were acquired at different stages to measure this process by locating the interface between water and soil sediment.

Apply the mixing formula (equation (4)) for the multi-layered system of water and sediment yields:

$$L_1\sqrt{K_{a,w}} + L_2\sqrt{K_{a,bs}} = L\sqrt{K_{a,m}} \quad (5)$$

where $K_{a,w}$ is the dielectric constant of water, which is commonly selected as 81; $K_{a,bs}$ is the dielectric constant of sand-water mixture in the sediment layer; $K_{a,m}$ is the measured bulk dielectric constant; L_1 , L_2 are the thickness of water layer and sand layer, respectively. L is the effective vertical length of the TDR probe, which equals to sum of water layer thickness and sand layer thickness for the experimental set up used in this study (Fig. 2).

Assume the thickness of sand layer in Fig. 2 is x , then $L_1 = L - x$. Substituting into equation (5), the following equation (6) can be obtained. If probe length, L , is a constant, the thickness of sediment, x , is linearly proportional to the square root of measured bulk dielectric constant. Therefore, the thickness of sediment can be predicted from TDR measured dielectric constants using equation (6).

$$x = \frac{\sqrt{K_{a,m}} - \sqrt{K_{a,w}}}{\sqrt{K_{a,bs}} - \sqrt{K_{a,w}}} L \quad (6)$$

DESIGN AND FABRICATION OF SPIRAL-SHAPED SENSOR

Figure 3 shows the design of a spiral TDR scour sensor. It is made of a square fiberglass rod as the mechanical mount and two conductive copper wires as TDR wave guide. The fiberglass rod is 500 mm in longitudinal length and 6 mm in cross-section length. The copper wires are 1 mm in diameter and wrapped in spiral around the central rod with wire spacing of 2 mm. The cross-section of central rod is selected as square shape so that fabrication grooves can be easily created along the fiberglass rod to assisting the control of wire spacing. The copper wires are coated by polyurethane insulating material. A commercial super-hydrophobic coating is sprayed on the surface of copper wire and core rod to eliminate the effects of residual water trapped between adjacent wires. The sensing component of the TDR probe used for this study is around 400 mm in length. It can be easily extended to different lengths based on specific applications. A BNC adapter is used to connect the spiral sensor and TDR system. The purpose of spiral shape of the TDR probe is to improve the sensitivity and resolution in detecting the interfaces along the direction of the probe. Fig. 3 also shows a two-rod straight probe, which has identical equivalent length to spiral probe. Two copper wires are fixed in parallel on the supportive rod with spacing of 3 mm.

CALIBRATION OF SPIRAL-SHAPED SENSOR

The measured dielectric constant by the TDR probe can be affected by the coating materials (Xiong 2003). Coating with lower dielectric constant can have a large impact on the measurement results. The mounting fiberglass rod may also affect the measured effective dielectric constant. These factors can be accounted for by calibration on materials with known dielectric constant.

Calibration with liquid

Four commonly used standard solvents and ethanol-DI water mixtures are employed to calibrate the spiral TDR probe. The standard solvents include deionized water (with dielectric constant of 80.4), methanol (33.1), ethanol (24.3), and acetone (20.7) (Lidström et al. 2001). Different amount of DI water is mixed with ethanol shown in Fig. 4 (b). The spiral sensor is totally submerged in these liquids and the TDR signals in each solution are acquired. The TDR signal in the air is also obtained as a control group. Fig. 4 illustrates the TDR signals of the spiral TDR sensor under different testing liquids. The black arrows shown in the figures represent the reflection points at the start and end of probe. The measured dielectric constant for each solution is calculated by using equation (3). The dielectric constant of ethanol-DI water mixture can be calculated using equation (4) with $\alpha = 1.0$. Fig. 5 shows relationship between measured results with spiral probe and actual dielectric constant by equation (4). By fitting the data in this figure, the calibration equation can be given by equation (7) with $R^2 = 0.99$, in which $K_{a,r}$, $K_{a,m}$ are the real dielectric constant of the liquid and the measured dielectric constant by coated TDR probe, respectively.

$$K_{a,r} = 0.7872K_{a,m}^3 - 22.143K_{a,m}^2 + 215.78K_{a,m} - 688.79 \quad (7)$$

Calibration with moisture soil

The dielectric constant of soil is closely related to its moisture content, since water has a much larger dielectric constant than that of soil particles or air (Drnevich et al. 2001; Siddiqui and Drnevich 1995; Topp and Davis 1985; Yu and Drnevich 2004). Siddiqui and Drnevich (1995) developed an empirical formula to explicitly correlate measured dielectric constant by TDR to the gravimetric water content, see equation (8), which is extensively adopted in geotechnical engineering.

$$\sqrt{K_a} \frac{\rho_w}{\rho_d} = a + bw \quad (8)$$

where ρ_d is the dry density of soil; ρ_w is the density of water; w is the gravimetric water content; K_a is the apparent dielectric constant. a and b are soil dependent calibration constants.

Sand with different water content is prepared and compacted in a stainless cylinder. The spiral probe is completely embedded in the moisture sand (Fig. 6). The density and water content of the sand is measured. TDR signals are obtained as shown in Fig. 7. With the increasing water content of soil, the travelling distance of EM wave in the soil increases. This is because the increasing water content results in increases of the soil dielectric constant. The dielectric constant of soil is computed using equation (3). The relationship between dielectric constant, dry density and water content of soil is plotted in the format of equation (8) and shown in Fig. 8. A highly linear relationship ($R^2 = 0.95$) is demonstrated between measured dielectric constant and soil properties with $a = 0.91$ and $b = 1.95$, respectively.

SIMULATED SCOURING TEST WITH NEW SPIRAL TDR SCOUR PROBE

Experimental program

TDR technology has been utilized for the bridge scour monitoring by Yankielun and Zabilansky (1999) and (Yu 2009). Bin et al. (2010) and Yu et al. (2013) conducted bridge scour experiments by traditional 3-rod and a distributed strip TDR sensor. Considering the resolution and sensitivity limitation of the sensor, the incremental thickness in the sedimentation layer during these previous studies were set around 4 cm and 10 cm, respectively.

To evaluate the performance of new sensor, simulated sedimentation/scour tests were implemented in the laboratory using the new spiral sensor. The tank was firstly fully filled with tap water with constant water level (39.6 cm in this study). Both the spiral and straight TDR probe (Fig. 3) were vertically installed in the tank. Dry soils were then gradually added into the tank to simulate the sedimentation process. TDR signals were acquired at different thickness of sediment layer. This process continued until the tank was fully filled with soils. Commercial Campbell CS 605 3-rod probe was also employed in the tests only with pure tap water and soils, which were used to calculate dielectric constant of tap water and saturated soils. The soils in the sediment layer were assumed saturated in this study. .

Testing materials

Two types of soils were prepared to simulate the sediments, i.e., coarse sand and fine sand. The grain size distributions are shown in Fig. 9.

Experiment results analysis

Fig. 10 shows TDR output signals of scour test for fine and coarse soils, including conventional straight and new spiral probe. The sediment layer is changed with 2 cm increment, which is one fifth of that Yu's (2009) experiment using a strip probe. The resultant TDR signals for spiral TDR probe are shown in Fig. 10 (a) and (c). Those for straight TDR probe are shown in Fig. 10 (b) and (d). With the increasing soil thickness, the dielectric constant of the overall system, $K_{a,m}$, decreases, giving rise to the decrease of the apparent length. An obvious observation is that with the same change in the sediment layer thickness, there are much more significant change in the travel time of EM wave (reflect at the end of the TDR probe) for the spiral TDR probe than the straight TDR probe.

The dielectric constant of water-soil mixture is computed based on the theory introduced in the previous context. $K_{a,r}$ is then obtained using calibration equation (7). Fig. 11 illustrates the measured dielectric constant of water-soil mixture versus sediment layer thickness in the format of equation (6). The square root of dielectric constant of water-soil mixture changes linearly with sediment layer thickness for both fine and coarse sediments. This is consistent with the relationship illustrated in equation (6). Therefore, the algorithm for scour depth estimation based on equation (6) can be used for the spiral TDR probe.

The dielectric constant of saturated soil and tap water used in this test program were obtained using commercial Campbell CS 605 3-rod probe, which is 69.9 and 20.77, respectively. Substituting the value of $K_{a,w}$, $K_{a,bs}$, $K_{a,m}$ and L into equation (6), the sediment layer thickness can be estimated from the dielectric constant measured by the spiral TDR probe.

Fig. 12 compares the physically measured sediment layer thickness by a ruler versus TDR predicted values for both fine and coarse grained sediments. The predicted values using the new spiral TDR sensor closely matches those of ruler measurements. This indicates that the new sensor can be employed to accurately estimate the scour depth or sediment layer thickness. The accuracy of the new sensor in predicting the sediment layer thickness falls within $\pm 5\%$, which is satisfactory for practical applications. The accuracy for fine sediment is significantly higher (generally within $\pm 2\%$).

The possible sources of experimental errors include: 1) the small diameter of copper waveguide implies a smaller effective sensing area, which might cause inaccuracy for sediments with larger grain as seen in Figure 12; 2) inaccurate measurement of sand layer thickness due to the difficulty to achieve a complete even surface; 3) errors in the determination of reflection points from TDR signals; 4) the dielectric constant of

water maybe not be exactly equal to that of tap water acquired by CS 605 sensor due to the turbidity of water layer, as discussed by Yu (2009).

Comparison with straight TDR scour probe

The sensitivity of a sensor is defined as the ratio of the magnitude of its response to the magnitude of measured quantity (Radatz 1997). To compare the sensitivity of the new spiral TDR probe versus that of a conventional straight TDR probe, Fig. 13 plots the effects of sediment layer thickness on the measured apparent length by the spiral and straight probes. The apparent length is highly linear with sediment layer thickness. There are, however, significant differences in the slope of the sensitivity curves by two different TDR probes. The slope of the sensitivity curve by the new spiral TDR sensor is about 4 times that of a regular straight TDR sensor probe. This implies that the spiral TDR probe is about 4 times more sensitive than straight TDR probe in scour depth determination. The sensitivity can be further improved by refining the spiral geometry design.

CONCLUSIONS

This paper describes the design and fabrication of an innovative spiral TDR scour sensor, which consists of copper wires TDR wave guide wrapped spirally around a mounting rod. The spiral sensor features higher sensitivity than the traditional probes due to the longer traveling distance of the EM wave per unit length along the direction of mounting rod. The performance of the spiral TDR probe is evaluated by calibration using liquid with known dielectric constant and soils with different moisture contents. Simulated scour experiments were conducted in the laboratory to evaluate the performance of the spiral TDR probe in monitoring the scouring process. The results show that the spiral TDR scour sensor easily detect the change of sediment layer thickness of less than 2cm. The square root of measured dielectric constant by the spiral TDR changes linearly with the sediment layer thickness (or scour depth). The estimated scour depth from the spiral TDR sensor agrees very well with that by direct ruler measurement. Compared with a straight TDR scour probe, the new spiral sensor is about 4 times more sensitive in detecting the scour depth. Besides, the sensitivity can be further improved by refining the spiral design.

ACKNOWLEDGEMENT

We acknowledge the support of Saada Family fellowship in the course of this study. This study is also partially supported by the U.S. National Science Foundation (0900401, 0846475). The assistance from Jim Berilla, department technician, is also highly appreciated.

REFERENCES

- Amirjahed, A., and Blake, M. I. (1974). "Relationship of composition of nonaqueous binary solvent systems and dielectric constant." *Journal of pharmaceutical sciences*, 63(1), 81-84.
- Anderson, N. L., Ismael, A. M., and Thitimakorn, T. (2007). "Ground-penetrating radar: a tool for monitoring bridge scour." *Environmental & Engineering*

- Geoscience*, 13(1), 1-10.
- Bin, Z., Xinbao, Y., and Xiong, Y. (2010). "Design and evaluation of a distributed TDR moisture sensor." *Smart Structures and Systems*, 6(9), 1007-1023.
- Birchak, J. R., Gardner, C., Hipp, J., and Victor, J. (1974). "High dielectric constant microwave probes for sensing soil moisture." *Proceedings of the IEEE*, 62(1), 93-98.
- Briaud, J.-L., Hurlebaus, S., Chang, K.-A., Yao, C., Sharma, H., Yu, O.-Y., Darby, C., Hunt, B. E., and Price, G. R. (2011). "Realtime monitoring of bridge scour using remote monitoring technology." Texas Transportation Institute, Texas A&M University System.
- Briaud, J., Chen, H., Li, Y., Nurtjahyo, P., and Wang, J. (2005). "SRICOS-EFA Method for Contraction Scour in Fine-Grained Soils." *J Geotech Geoenviron*, 131(10), 1283-1294.
- Briaud, J., Ting, F., Chen, H., Cao, Y., Han, S., and Kwak, K. (2001). "Erosion Function Apparatus for Scour Rate Predictions." *J Geotech Geoenviron*, 127(2), 105-113.
- Chien, Y. W. (1984). "Solubilization of metronidazole by water-miscible multi-cosolvents and water-soluble vitamins." *PDA Journal of Pharmaceutical Science and Technology*, 38(1), 32-36.
- De Falco, F., and Mele, R. (2002). "The monitoring of bridges for scour by sonar and sediment." *NDT & E International*, 35(2), 117-123.
- Drnevich, V., Lin, C., Yi, O., and Lovell, J. (2001). "Real-Time Determination of Soil Type, Water Content, and Density Using Electromagnetics." *Joint Transportation Research Program*, 177.
- Drnevich, V. P., Siddiqui, S. I., Lovell, J., and Yi, Q. "Water content and density of soil insitu by the purdue TDR method." *Proc., Second International Symposium on Time Domain Reflectometry*.
- Dumanovic, D., Kosanovic, D., Mrdakovic, D., and Jovanovic, J. (1992). "Solubilization of ipronidazole by co-solvents." *Pharmazie*, 47(8), 603-607.
- Forde, M. C., McCann, D. M., Clark, M. R., Broughton, K. J., Fenning, P. J., and Brown, A. (1999). "Radar measurement of bridge scour." *NDT & E International*, 32(8), 481-492.
- Hayes, D. C., and Drummond, F. (1995). *Use of fathometers and electrical-conductivity probes to monitor riverbed scour at bridge piers*, US Department of the Interior, US Geological Survey.
- Hunt, B. (2009). "Monitoring Scour Critical Bridges: A Synthesis of Highway Practice." *NCHRP Synthesis Report*, 396.
- Joshi, Y. S., Hudge, P. G., Kumbharkhane, A. C., and Mehrotra, S. C. (2011). "The dielectric relaxation study of 2(2-alkoxyethoxy)ethanol–water mixtures using time domain reflectometry." *Journal of Molecular Liquids*, 163(2), 70-76.
- Jouyban, A., Soltanpour, S., and Chan, H.-K. (2004). "A simple relationship between dielectric constant of mixed solvents with solvent composition and temperature." *International journal of pharmaceuticals*, 269(2), 353-360.
- King, M. B., and Queen, N. M. (1979). "Use of rational functions for representing

- data." *Journal of Chemical and Engineering Data*, 24(3), 178-181.
- Ledieu, J., De Ridder, P., De Clerck, P., and Dautrebande, S. (1986). "A method of measuring soil moisture by time-domain reflectometry." *Journal of Hydrology*, 88(3), 319-328.
- Lefter, J. (1993). "Instrumentation for measuring scour at bridge piers and abutments." *NCHRP Research Results Digest*(189).
- Lidström, P., Tierney, J., Wathey, B., and Westman, J. (2001). "Microwave assisted organic synthesis—a review." *Tetrahedron*, 57(45), 9225-9283.
- Lin, Y.-B., Chen, J.-C., Chang, K.-C., Chern, J.-C., and Lai, J.-S. (2005). "Real-time monitoring of local scour by using fiber Bragg grating sensors." *Smart materials and structures*, 14(4), 664.
- Lin, Y. B., Chang, K. C., Lai, J.-S., and Wu, I.-W. "Applications of optical fiber sensor on local scour monitoring." *Proc., Sensors, 2004. Proceedings of IEEE, IEEE*, 832-835.
- Mason, R. R., and Sheppard, D. M. "Field performance of an acoustic scour-depth monitoring system." *Proc., Fundamentals and Advancements in Hydraulic Measurements and Experimentation, ASCE*, 366-375.
- Prakongpan, S., and Nagai, T. (1984). "Solubility of acetaminophen in cosolvents." *Chemical and pharmaceutical bulletin*, 32(1), 340-343.
- Prendergast, L. J., and Gavin, K. (2014). "A review of bridge scour monitoring techniques." *Journal of Rock Mechanics and Geotechnical Engineering*, 6(2), 138-149.
- Radatz, J. (1997). *The IEEE standard dictionary of electrical and electronics terms*, IEEE Standards Office.
- Radchenko, A., Pommerenke, D., Chen, G., Maheshwari, P., Shinde, S., Pilla, V., and Zheng, Y. R. "Real time bridge scour monitoring with magneto-inductive field coupling." *Proc., SPIE Smart Structures and Materials+ Nondestructive Evaluation and Health Monitoring*, International Society for Optics and Photonics, 86922A-86922A-86915.
- Siddiqui, S., and Drnevich, V. (1995). *A new method of measuring density and moisture content of soil using the technique of time domain reflectometry*, Joint Highway Research Project, Purdue University.
- Sohn, H., Farrar, C. R., Hemez, F. M., Shunk, D. D., Stinemates, D. W., Nadler, B. R., and Czarnecki, J. J. (2004). *A review of structural health monitoring literature: 1996-2001*, Los Alamos National Laboratory Los Alamos, NM.
- Topp, G. C., and Davis, J. L. (1985). "Measurement of Soil Water Content Using Time Domain Reflectometry (TDR): A Field Evaluation." *Soil Sci Soc Am J*, 49, 3.
- Xiong, W., Cai, C., and Kong, X. (2012). "Instrumentation design for bridge scour monitoring using fiber Bragg grating sensors." *Applied optics*, 51(5), 547-557.
- Xiong, Y. (2003). "Influence of soil properties and environmental conditions on electromagnetic wave propagation in soils."
- Yankielun, N., and Zabilansky, L. (1999). "Laboratory Investigation of Time-Domain Reflectometry System for Monitoring Bridge Scour." *Journal of Hydraulic*

Engineering, 125(12), 1279-1284.

Yu, X. (2009). "Experimental Study of an Innovative Bridge Scour Sensor." Case Western Reserve University.

Yu, X., and Drnevich, V. P. (2004). "Soil water content and dry density by time domain reflectometry." *J Geotech Geoenviron*, 130(9), 922-934.

Yu, X., and Zabilansky, L. J. (2006). "Time Domain Reflectometry for Automatic Bridge Scour Monitoring." *Site and Geomaterial Characterization*, 152.

Yu, X. Y., Zhang, B., Tao, J., and Yu, X. (2013). "A new time-domain reflectometry bridge scour sensor." *Structural Health Monitoring*, 12(2), 99-113.

Zabilansky, L. J. (1996). "Ice Force and Scour Instrumentation for the White River, Vermont." DTIC Document.

LIST OF FIGURES

Fig. 1 a) Schematic diagram of a typical TDR system; b) An example of TDR output signal (Drnevich et al. 2001)

Fig. 2 Schematic diagram of soil-water mixture

Fig. 3 Comparison of straight TDR probe and spiral-shaped TDR probe

Fig. 4 Output signals of spiral sensor in liquid (a- in standard solvent; b- in ethanol-DI water mixture)

Fig. 5 Relationship between measured and real dielectric constant

Fig. 6 Calibration of spiral TDR probe with moisture sand

Fig. 7a Output signals of TDR with spiral probe in moisture sand

Fig. 8 Calibration of spiral probe with moisture sand

Fig. 9 Grain size distribution of testing materials

Fig. 10 TDR output signals for fine and coarse soil (a – spiral probe in fine sand; b – straight probe in fine sand; c – spiral probe in coarse sand; d – straight probe in coarse sand)

Fig. 11 Relationship between dielectric constant and sediment thickness (a - fine soil; b – coarse soil)

Fig. 12 Measured and predicted sediment layer thickness (a - fine sediment; b – coarse sediment)

Fig. 13 Relationship between sediment layer thickness and apparent length

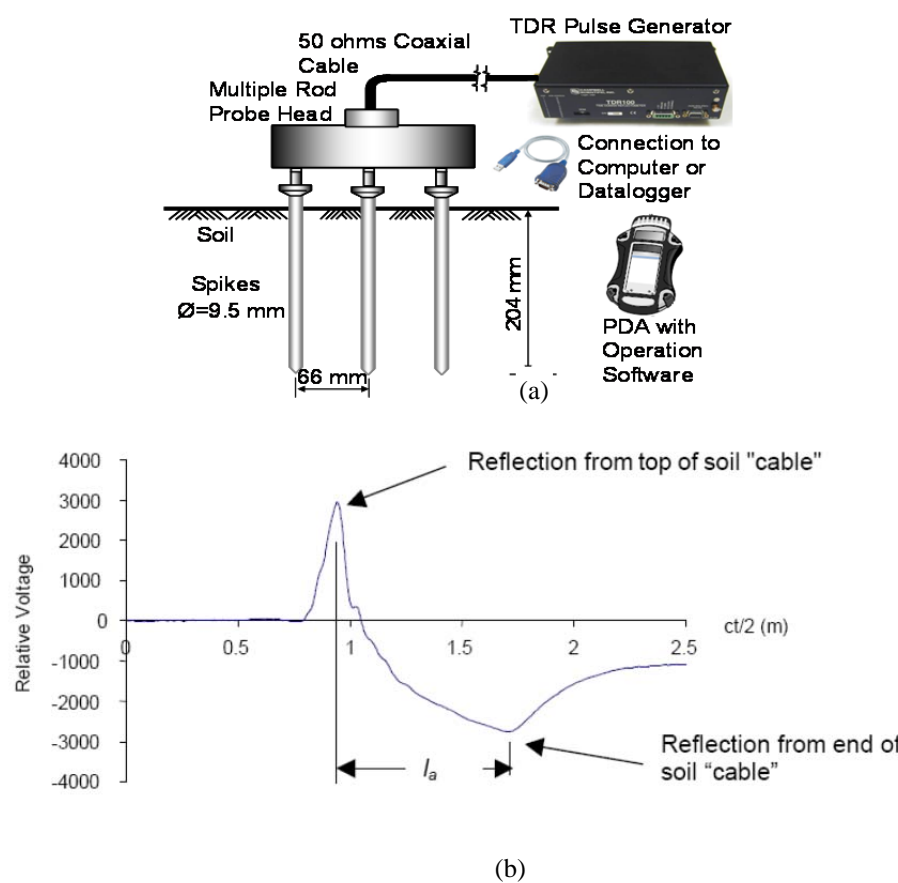


Fig. 1 a) Schematic diagram of a typical TDR system; b) An example of TDR output signal (Drnevich et al. 2001)

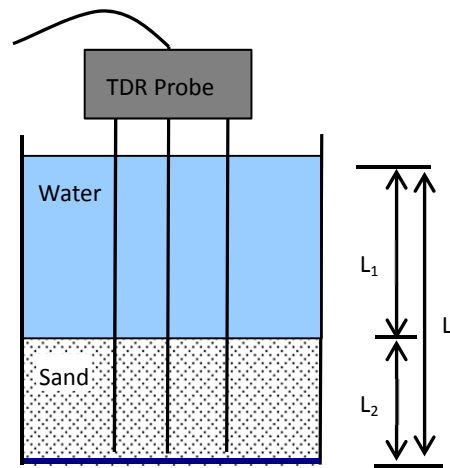


Fig. 2 Schematic diagram of soil-water mixture

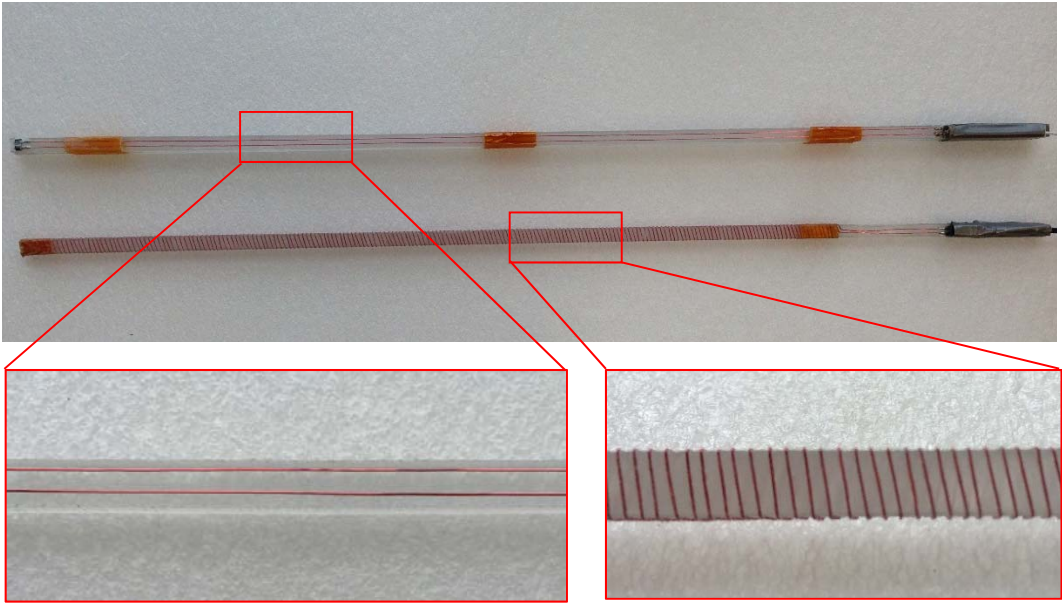


Fig. 3 Comparison of straight TDR probe and spiral-shaped TDR probe

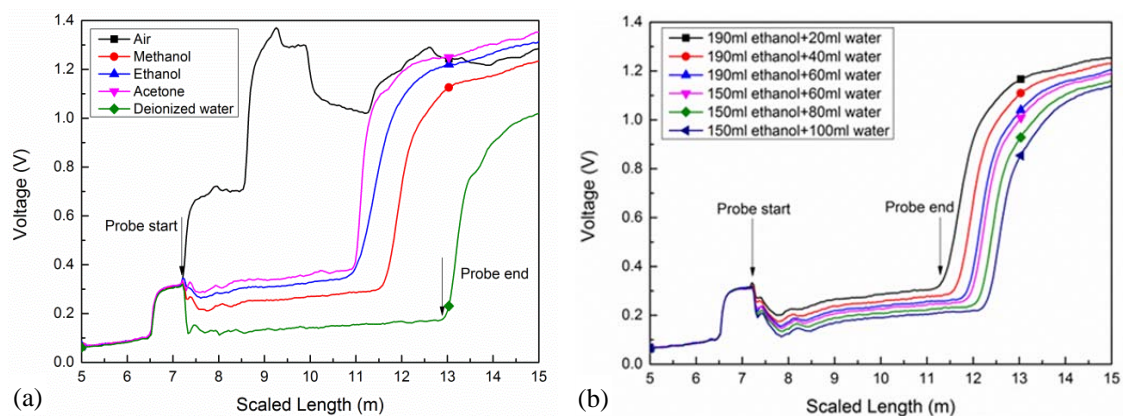


Fig. 4 Output signals of spiral sensor in liquid (a- in standard solvent; b- in ethanol-DI water mixture)

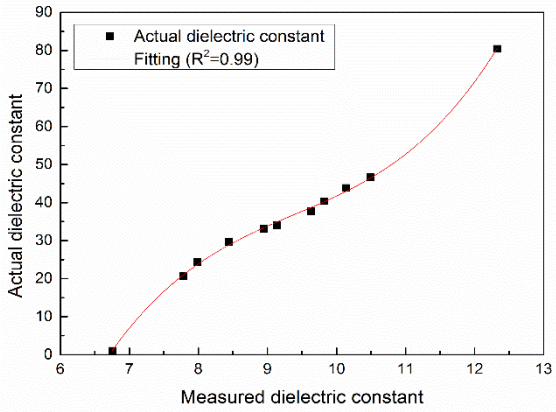


Fig. 5 Relationship between measured and real dielectric constant



Fig. 6 Calibration of spiral TDR probe with moisture sand

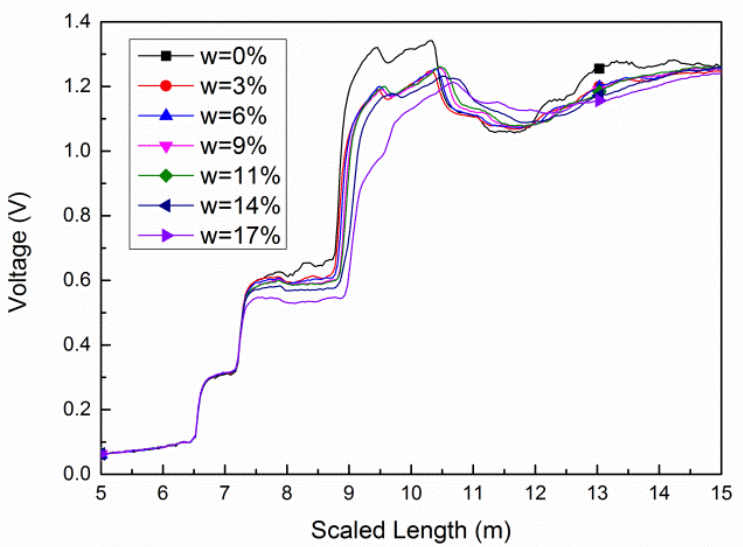


Fig. 7a Output signals of TDR with spiral probe in moisture sand

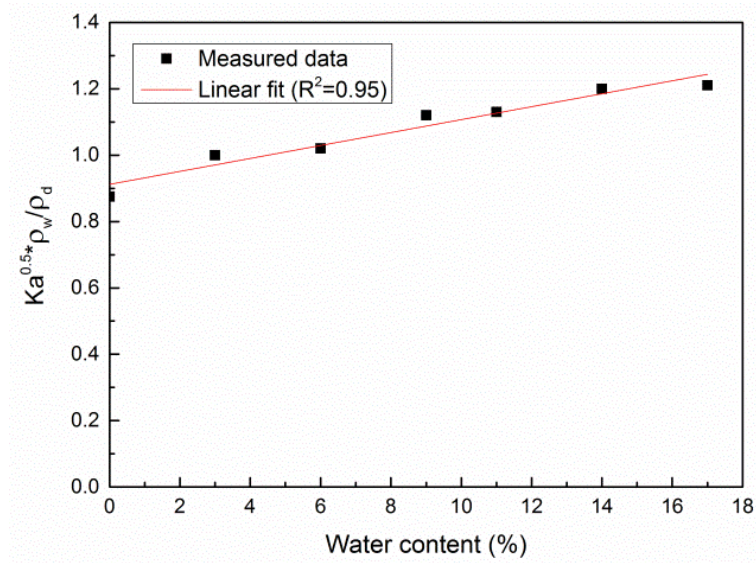


Fig. 8 Calibration of spiral probe with moisture sand

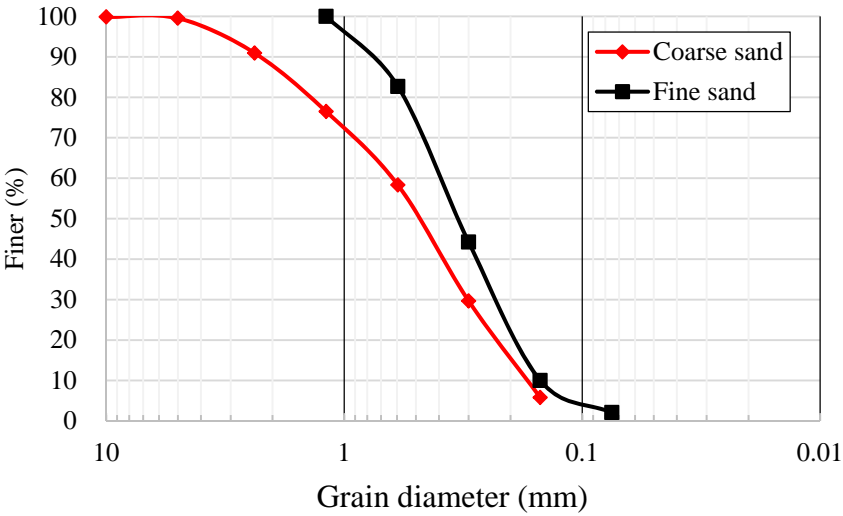
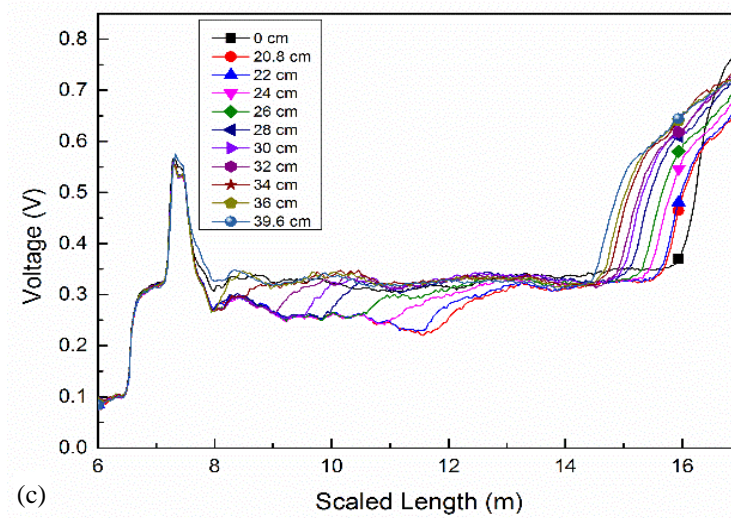
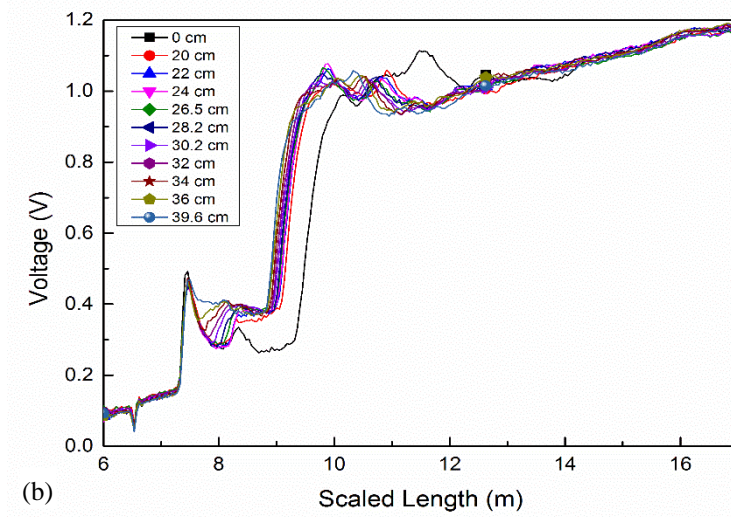
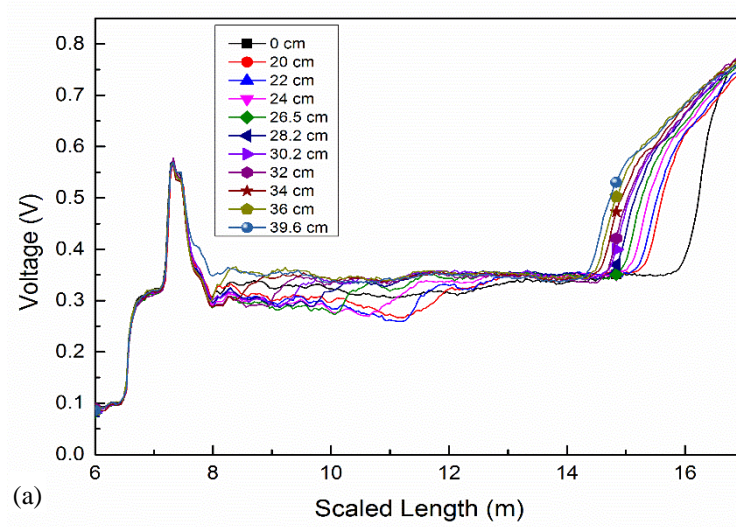


Fig. 9 Grain size distribution of testing materials



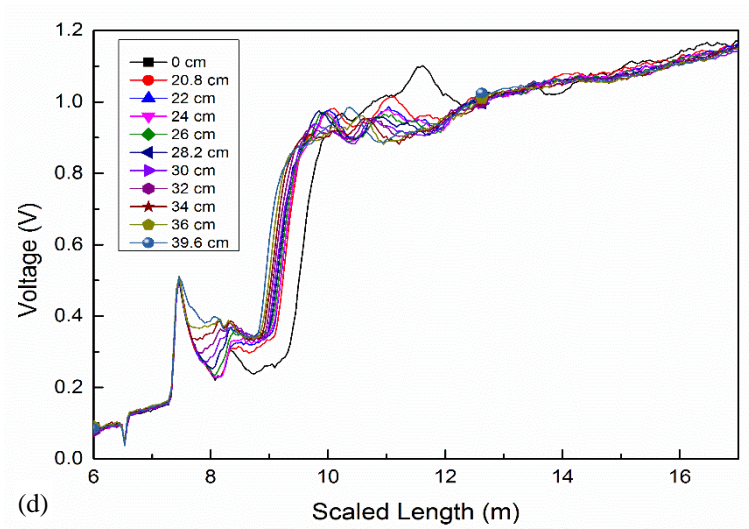


Fig. 10 TDR output signals for fine and coarse soil (a – spiral probe in fine sand; b – straight probe in fine sand; c – spiral probe in coarse sand; d – straight probe in coarse sand)

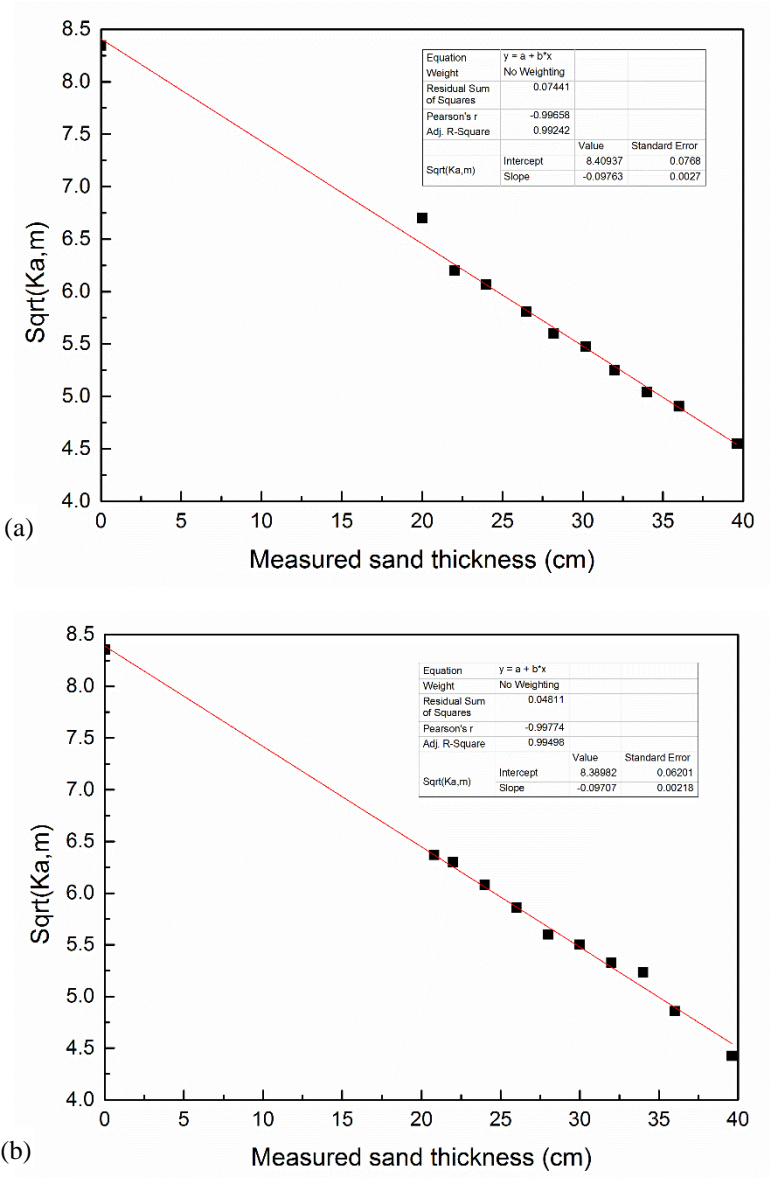


Fig. 11 Relationship between dielectric constant and sediment thickness (a - fine soil; b – coarse soil)

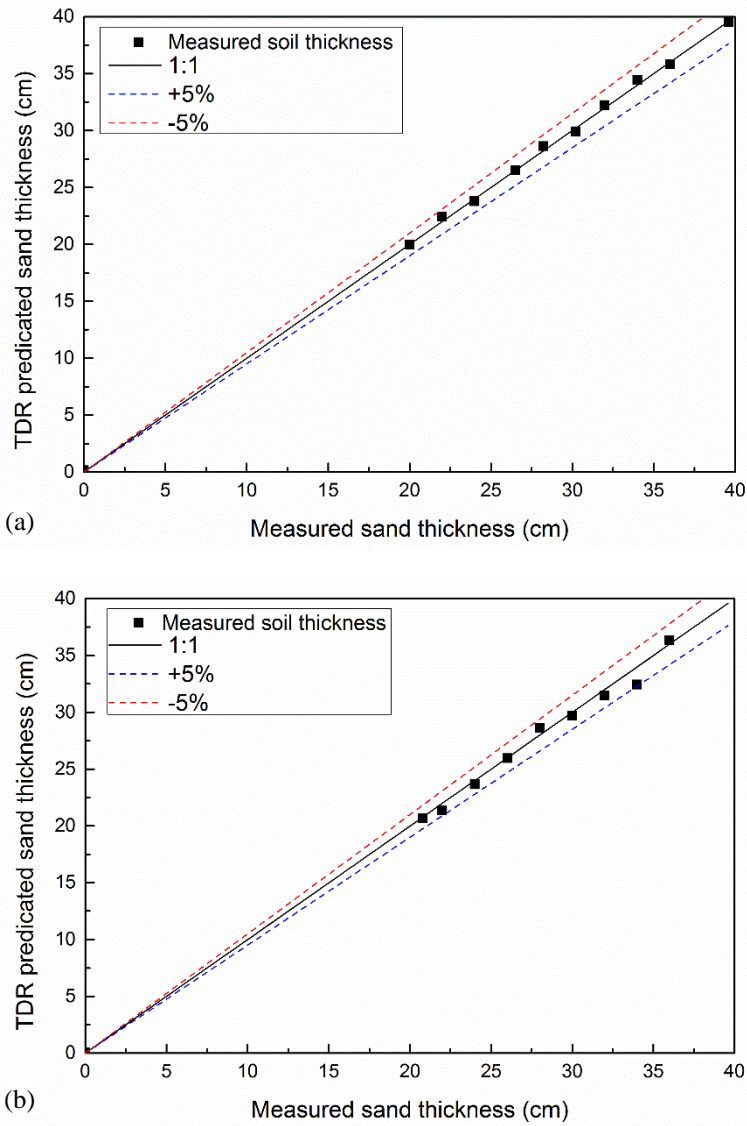


Fig. 12 Measured and predicted sediment layer thickness (a - fine sediment; b – coarse sediment)

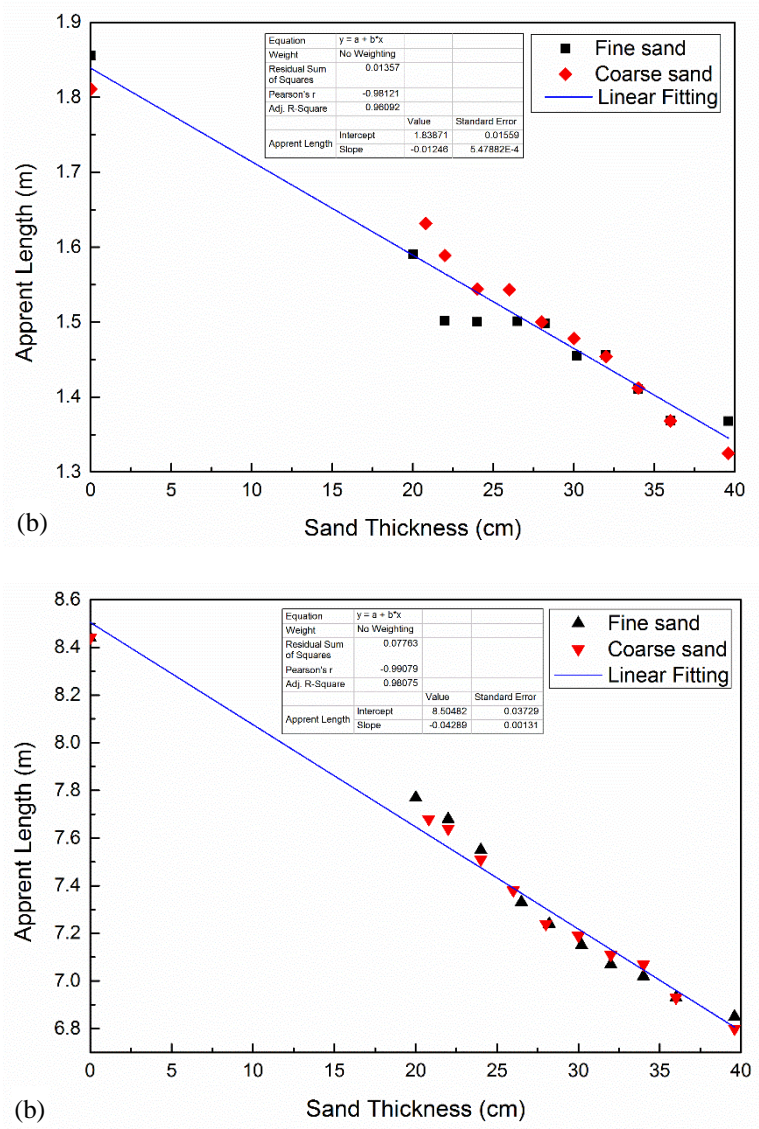


Fig. 13 Relationship between sediment layer thickness and apparent length (a – straight probe; b – spiral probe)